

This article was downloaded by:

On: 25 January 2011

Access details: *Access Details: Free Access*

Publisher *Taylor & Francis*

Informa Ltd Registered in England and Wales Registered Number: 1072954 Registered office: Mortimer House, 37-41 Mortimer Street, London W1T 3JH, UK



Separation Science and Technology

Publication details, including instructions for authors and subscription information:

<http://www.informaworld.com/smpp/title~content=t713708471>

Sedimentation and Filtration Equilibria

D. E. Smiles^a

^a DIVISION OF ENVIRONMENTAL MECHANICS, CSIRO, CANBERRA CITY, A.C.T., AUSTRALIA

To cite this Article Smiles, D. E. (1976) 'Sedimentation and Filtration Equilibria', *Separation Science and Technology*, 11: 1, 1 – 16

To link to this Article: DOI: 10.1080/01496397608085297

URL: <http://dx.doi.org/10.1080/01496397608085297>

PLEASE SCROLL DOWN FOR ARTICLE

Full terms and conditions of use: <http://www.informaworld.com/terms-and-conditions-of-access.pdf>

This article may be used for research, teaching and private study purposes. Any substantial or systematic reproduction, re-distribution, re-selling, loan or sub-licensing, systematic supply or distribution in any form to anyone is expressly forbidden.

The publisher does not give any warranty express or implied or make any representation that the contents will be complete or accurate or up to date. The accuracy of any instructions, formulae and drug doses should be independently verified with primary sources. The publisher shall not be liable for any loss, actions, claims, proceedings, demand or costs or damages whatsoever or howsoever caused arising directly or indirectly in connection with or arising out of the use of this material.

Sedimentation and Filtration Equilibria

D. E. SMILES

DIVISION OF ENVIRONMENTAL MECHANICS
CSIRO
CANBERRA CITY, A.C.T. 2601, AUSTRALIA

Abstract

A theory to describe transient and static equilibrium profiles in sedimentation and filtration is proposed. The dynamic aspects are based on Darcy's law and a continuity requirement in Lagrangian coordinates, recognizing that the Darcy flux describes flow of liquid relative to the particles in response to a space gradient of liquid potential. The equilibrium profiles may be calculated when the space gradient of liquid potential is zero. The theory is restricted to materials where the particle size distribution is such that no sorting of particles occurs.

Equilibrium profiles are calculated for a red-mud effluent produced following extraction of alumina from bauxite, and experimental data consistent with the theory presented.

Some gravity-driven dewatering strategies are discussed.

Many mining industries are faced with the disposal of large volumes of slurries. This problem can often be ameliorated if a feasible method of separating the solid and liquid components is available. The liquid may then be reused and the solid stabilized to provide a satisfactory base for landscape recovery.

In many instances the volumes of these effluents are so great that conventional methods of separation, such as centrifugation, pressure filtration, and oven drying, are impracticable and the industry is restricted to processes in which gravity provides the driving force. Probably the most significant gravity-driven process is sedimentation, and yet it remains poorly understood.

This paper draws attention to a theory that permits prediction of some aspects of sedimentation. Also, the efficacy of sedimentation is compared with that of "self-weight" filtration, an alternative gravity-driven process.

Conventional approaches to sedimentation are based in general either on Stokes' law for materials that are not subject to Brownian motion or on a diffusion-type theory if the particles are sufficiently small. It is central to both approaches that the motion of the particles be described. Equilibrium in a gravitational field occurs when Stokesian settling is balanced by an upward flux due to the particle concentration gradient.

In the theory presented here, we examine the process in terms of the transfer of the *liquid relative to the solid*. This differs from the conventional approach originating in Stokes-type analyses, for example, in Refs. 1-3 and, of course, recognizes and accounts for liquid/solid interaction, where a Stokes' law approach appears not to be very useful. Batchelor (4), for example, attempts an approach based on microscopic flow about adjacent spheres without developing a macroscopic theory. He also mentions that Darcy's law might be useful for predicting flow about sedimenting particles, but curiously fails to explore the use of Darcy's law to describe macroscopic flow of liquid in the sedimenting system.

In addition, we examine the process in the context of a material within which the particle size distribution and concentration are such that sorting does not occur. This assumption is common in theoretical treatments of sedimentation (1, 3), and implies that we can relate the liquid content, θ , of the medium to an interparticle stress, or liquid potential, Ψ . Ψ represents the work per unit weight of liquid that must be done against capillary and absorptive forces associated with the solid particles and their geometry in order to remove an element of liquid to a pool at the same height in the gravitational field.

Practically, Ψ may be defined in terms of the manometric pressure, p_1 , measured across a membrane that permits the passage of liquid but not solid, and the total pressure P , by

$$\Psi + p_1 = P = \int_z^T \gamma dz \quad (1)$$

where z is the vertical axis positive upwards, γ is the wet specific gravity of the system, and T is its upper surface.

This statement is consistent with the effective stress principle of soil mechanics literature when applied to saturated soil (see, for example, Refs. 5 and 6). In engineering terminology, Ψ is minus the effective or interparticle stress, and p_1 is the pore pressure. A full statement of the concepts involved, in soil-physical terms, is presented by Philip (7, 8).

In such a system, the vertical volume flux, v , of liquid relative to solid is described by Darcy's law,

$$v = -K \partial\Phi/\partial z \quad (2)$$

in which K , the hydraulic conductivity, is an experimentally determinable function of ϑ , and the total liquid potential, Φ , is given by

$$\Phi = z - Z + p_1 \quad (3)$$

where Z is a convenient height datum.

The introduction of a material coordinate, m , defined by

$$dm/dz = (1 + \vartheta)^{-1} \quad (4)$$

permits us to write a continuity statement in the form

$$(\partial\vartheta/\partial t)_m = -(\partial v/\partial m), \quad (5)$$

Further substitution of Eqs. (1)–(3) in Eq. (5) gives rise to a nonlinear Fokker-Planck equation,

$$\frac{\partial\vartheta}{\partial t} = \frac{\partial}{\partial m} \left[D_m \frac{\partial\vartheta}{\partial m} \right] + (\rho_c - 1) \frac{dK_m}{d\vartheta} \frac{\partial\vartheta}{\partial m} \quad (6)$$

In Eq. (6),

$$D_m = K_m d\Psi/d\vartheta = K/(1 + \vartheta) d\Psi/d\vartheta \quad (7)$$

and ρ_c is the solid specific gravity. The predictive use of Eq. (6) demands a knowledge of $K(\vartheta)$, $\Psi(\vartheta)$, and ρ_c . In general, it is not possible to predict these functions, but they are not difficult to determine experimentally. A suitable method using a small pressure-filtration cell is described by Smiles and Harvey (9). The development of Eqs. (1)–(7) has been described in more detail in a number of publications (for example, see Refs. 10–12). The last authors also tested the theory using homoionic bentonite for ϑ in the range $6 < \vartheta < 60$. Red mud produced as an effluent by the aluminium industry, and phosphate slime produced during extraction of rock phosphate also demonstrate transient liquid flow behavior that is consistent with this theory.

In this paper we will examine the use of the total potential function and experimental data on $\Psi(\vartheta)$ and ρ_c to predict equilibrium distributions of solid and liquid during sedimentation and self-weight filtration. The results suggest strategies for optimizing the separation process.

It is convenient to base the analysis on a column of slurry with an initially uniform liquid content, ϑ_n , and depth, T_n . According to Eq. (4), it will contain $M \text{ m}^3/\text{m}^2$ of solid, where $M = (1 + \vartheta_n)^{-1} T_n$. Also, we assume

that the density of the liquid is 10^3 kg/m^3 . The extension to other liquids is obvious.

We shall examine the liquid and solid profiles that arise when this column equilibrates with a free water surface set at Z relative to the base of the column (where we define $z = 0$) through a membrane that permits the passage of the liquid but not the solid. When Z approaches the column top, conditions are appropriate to sedimentation; when Z tends to 0, we have conditions appropriate to self-weight filtration. This is shown diagrammatically in Fig. 1. For this situation, the total potential of the liquid is given by

$$\Phi = \Psi + z + \int_z^T \gamma dz \quad (8)$$

But $\gamma = (\theta + \rho_c)/(\theta + 1)$, so Eq. (8), using Eq. (4), becomes

$$\Phi = \Psi + T + (\rho_c - 1)(M - m) \quad (9)$$

At static equilibrium, however, $\Phi = Z$ so

$$-\Psi = T - Z + (\rho_c - 1)(M - m) \quad (10)$$

This equation, which is analogous to Buckingham's equation (13) describing static equilibrium of water in a nonswelling soil, demonstrates that $-\Psi$ is a linear function of m with slope $-(\rho_c - 1)$ and intercept $(T - Z + [\rho_c - 1]M)$. For constant M , Ψ becomes more negative and the column

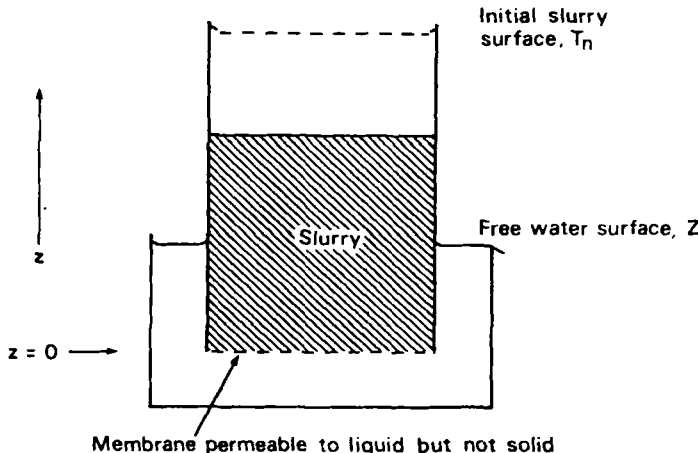


FIG. 1. Diagram showing the physical situation discussed in the text of a slurry equilibrating with an imposed constant free water surface.

drier throughout as $(T - Z)$ increases. A knowledge of $\Psi(\vartheta)$ then permits us to calculate various profiles. For example:

- (i) $\vartheta(m)$ for $0 \leq m \leq M$ follows directly from Eq. (10).
- (ii) $z(m)$ may be determined from

$$z = \int_0^m (1 + \vartheta) dm \quad (11)$$

for $0 \leq m \leq M$, using $\vartheta(m)$.

- (iii) $z(-\Psi)$ may be calculated using

$$-z = \int (1 + \vartheta)/(\rho_c - 1) d(-\Psi) \quad (12)$$

for appropriate limits of $-\Psi$.

- (iv) $z(\vartheta)$ may be calculated using

$$z = \int (1 + \vartheta) \frac{dm}{d\vartheta} d\vartheta \quad (13)$$

for appropriate limits on ϑ .

The limits to the integrals in Eqs. (12) and (13) emerge with the calculated equilibrium profile, the point being that the water-content profile, the suction profile, and the total amount of solid in the column must be mutually consistent. For a two-phase system there is only one profile that satisfies these requirements. A convenient approach is to calculate

$$z = \int_{T - Z + (\rho_c - 1)M}^{T - Z + (\rho_c - 1)(M - m)} (1 + \vartheta)/(\rho_c - 1) d(-\Psi) \quad (14)$$

This equation ensures that we conserve the original volume of solid, since M occurs in both limits of the integral. Thus if one plots

$$F(t) = \int_{T - Z + (\rho_c - 1)M}^{T - Z} (\vartheta + 1)/(\rho_c - 1) d(-\Psi) - T$$

interpolation gives the value of T for which $F = 0$. $T - Z$ is then defined, and $\Psi(z)$, and hence $\vartheta(z)$, may be calculated.

ILLUSTRATIVE EXAMPLE

Figure 2 shows $\vartheta(-\Psi)$ for a sample of red mud supplied by Comalco Aluminium (Bell Bay) Ltd., Tasmania, Australia. The data were obtained

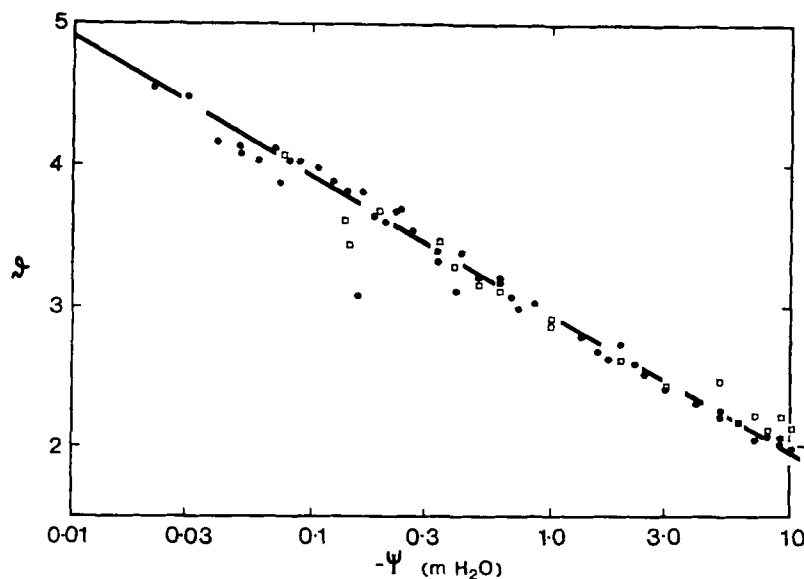


FIG. 2. Relationship between the water content, ϑ , and the unloaded water potential, Ψ , of a sample of red mud.

using the method described in Ref. 9. It is evident that within the ranges shown they can be described by an equation of the form

$$\vartheta = \alpha + \beta \ln(-\Psi/100) \quad (15)$$

in which $\alpha = 4.87$ and $\beta = -0.424$.

Figure 3 shows the way ϑ varies with z for this material. This figure was calculated using Eq. (13) together with Eqs. (10) and (15). All equilibrium profiles for this material lie on this curve, with the appropriate limits being the result of a particular set of values of M and Z . The limits may be found using Eq. (14).

Figure 4 shows a series of profiles of ϑ calculated for a column of red mud with $M = 100$ cm and a range of values for $T - Z$. The top of the z axis is the height of the equilibrium slurry when $T - Z = 0$. The ϑ profile corresponding to this condition is represented by the curve on the right-hand side limiting the family for $T - Z > 0$. The top of this limiting curve is at $z = 4.007$ m. Figure 5 shows the corresponding $(1 + \vartheta)^{-1}$ profiles. This last figure may be interpreted as a phase diagram showing the space

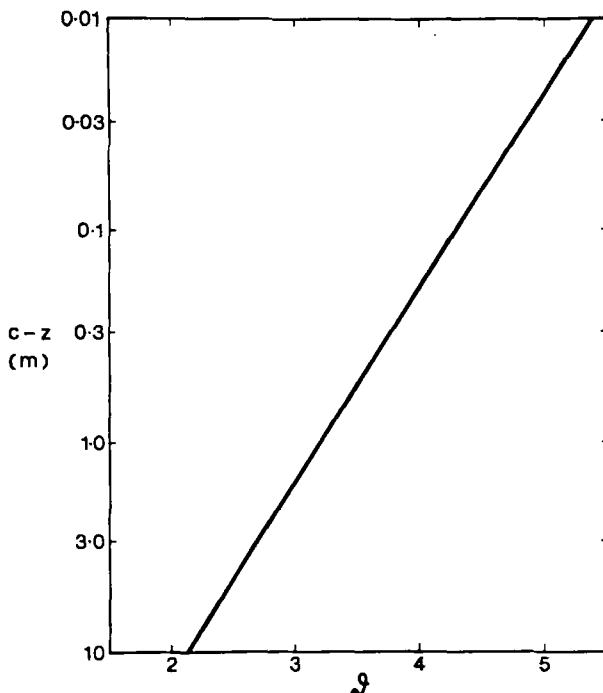


FIG. 3. The general relation between water content, θ , and depth for a column of red mud at equilibrium. c is an integration constant representing the upper surface of the sediment. All equilibrium profiles lie somewhere on this curve.

distribution of water and solid, since $(1 + \theta)^{-1}$ is the volume of solid per unit volume of slurry.

The dashed lines in Figs. 4 and 5 show the way the slurry surface at equilibrium must change with $(T - Z)$. The quantity of liquid recovered for each situation is the difference in height between this equilibrium surface and the initial depth, T_n .

Figures 4 and 5 both demonstrate that the efficacy of the gravity-driven dewatering process is increased as $(T - Z)$ is increased. In passing, it should be noted that the profile corresponding to $(T - Z) = 3.00$ m approximates that anticipated for this material when it is permitted to drain with the free water surface maintained at its base.

Having demonstrated the way equilibrium profiles at constant M depend

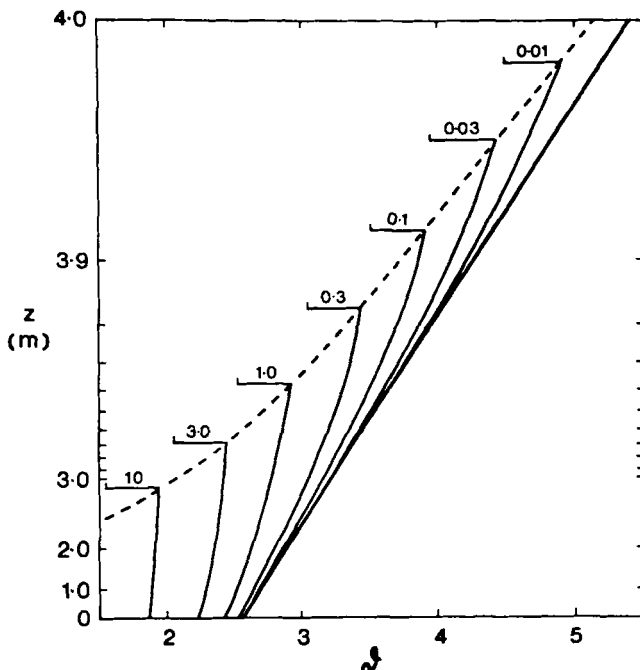


FIG. 4. A family of equilibrium $\vartheta(z)$ profiles expected in a column of red mud in which $M = 1$ m and $T - Z$ (the value of $-\Psi$ at the top of the sediment) is varied from 0 to 10 m. The right-hand curve represents the situation where $T - Z = 0$; its top is at 4.007 m.

upon $(T - Z)$, it is interesting to examine the effect of variation in M holding $(T - Z)$ constant. Figure 6 shows the way the average water content $\bar{\vartheta}$ [= $(T/M) - 1$] of a profile at equilibrium varies with M when $T = Z$ and $Z = 0$. We see that the recovery of water increases as M is increased, and that increasing $T - Z$ is always advantageous.

Figures 4, 5, and 6 demonstrate general patterns of equilibrium behavior for a red mud with $\Psi(\vartheta)$ of the form shown in Fig. 2. Their interpretation, particularly in the case of "sedimentation," requires some care. Sedimentation, in practice, involves placing a slurry in a container closed at the base. The solid and water components redistribute until $\partial\Phi/\partial z = 0$, but it does not follow immediately that free water will emerge at the top. For example, if $M = 1$ m but T_n were 3 m, the $\vartheta(z)$ profile would match exactly that observed for self-weight filtration with $Z = 0$, that is, with a surface value

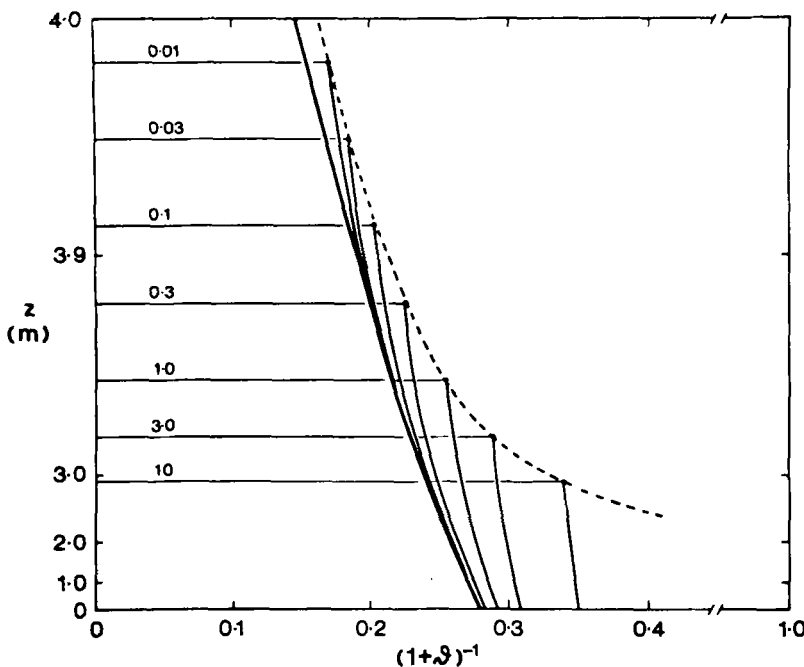


FIG. 5. Phase diagram showing the space liquid/solid distribution corresponding to the curves of Fig. 4. $(1 + \vartheta)^{-1}$ is the volume of solid per total volume of the two-phase system.

of Ψ of about -3 m; were $T_n \doteq 4$ m, the surface value of Ψ would be zero. Were T_n greater than 4 m, then the equilibrium solid distribution still has an upper surface at about 4 m, but clear water stands above it to T_n m. The relative efficacy of different treatments can thus be compared only in slurries defined in terms of T_n , ϑ_n , and, by implication, M .

EXPERIMENTAL

Equilibrium profiles do not necessarily provide a satisfactory basis for comparison between theory and experiment. This is because the final stages of the dewatering process are characterized by diminishing values of hydraulic conductivity and vanishing potential gradients, so in practice, one can observe only the approach of equilibrium.

Ultimately the test of the theory must be based on a satisfactory predic-

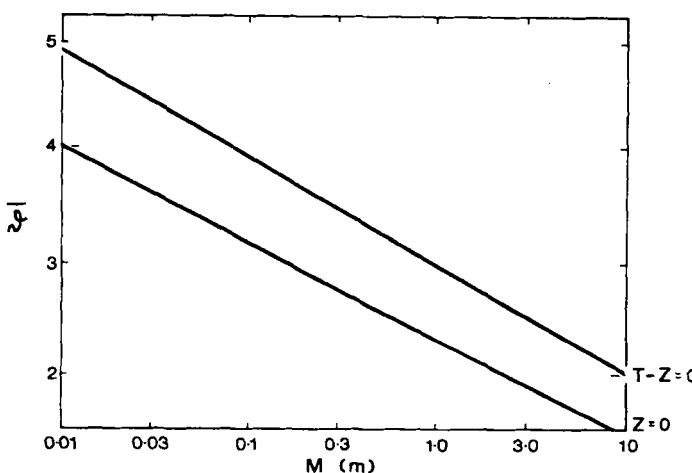


FIG. 6. The effect of M on the average equilibrium water content, $\bar{\vartheta}$, for two columns with $T - Z = -\Psi_{top} = 0$ and $-\Psi_{top} = T(Z = 0)$.

tion of the transient moisture profiles using solutions to Eq. (6). These solutions have yet to be developed although the problem, in principle, is reasonably straightforward in terms of boundary conditions. Some aspects of the process will be demonstrated in a following paper.

In order to speed the processes of sedimentation and self-weight filtration, a centrifuge was constructed. This machine spins a cylinder of slurry with the axis perpendicular to that of the centrifuge and at a mean distance of 1.1 m from it. The sample cylinder is approximately 0.15 m long and constructed so that it can be sectioned and the profiles of water content determined gravimetrically. The cylinder has an internal diameter of 4.1×10^{-2} m. Because of the distance from the axis and the length of the cylinder, the gravitational acceleration when the centrifuge rotates is assumed to be constant (≈ 120 to 145 g), and the parallel walls of the cylinder are assumed, to a reasonable approximation, to be parallel with the radius of the centrifuge along the cylinder axis. This assumption permits us to use the one-dimensional analysis set out above, but with an appropriately modified gravity term.

The sample cylinder could be used either with a sealed base (sedimentation) or with a membrane in the bottom through which liquid could escape (self-weight filtration).

Moisture profiles were determined with this device after 0.5 and 4 hr for both sedimentation and self-weight filtration. Figure 7(a) shows the pro-

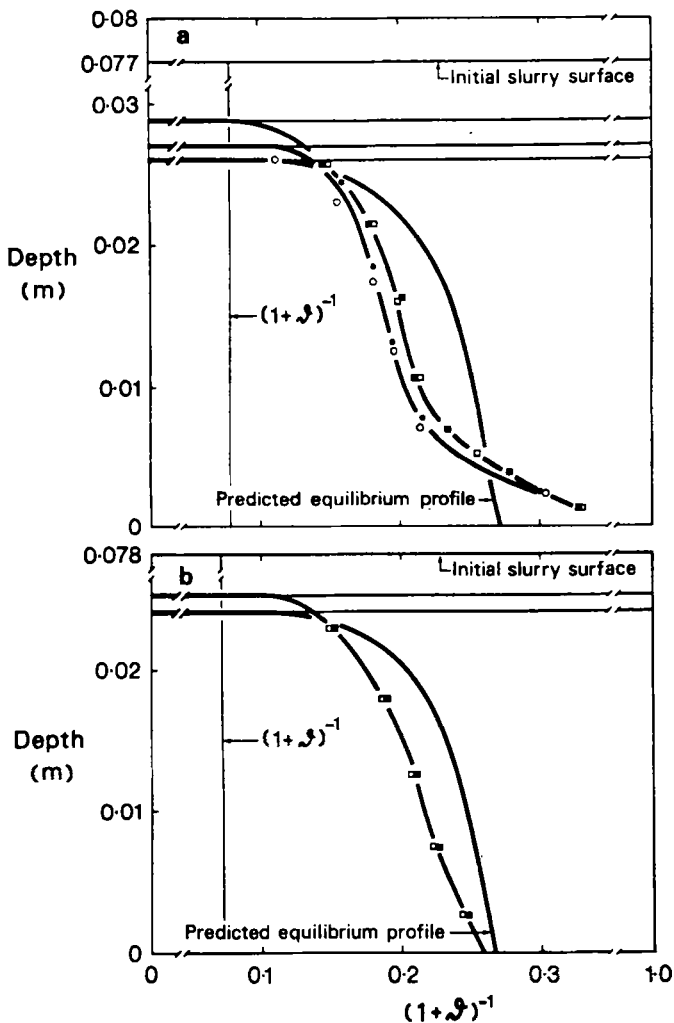


FIG. 7. Predicted and experimental solid/liquid profiles in a centrifuged sedimenting column. (○, ●) 30 min experimental data; (□, ■) 4 hr experimental data. Other details are described in the text.

files for sedimentation, expressed in terms of $(1 + g)^{-1}$, together with the equilibrium profile predicted using Fig. 2 and the theory set out above, assuming a gravitational acceleration of 136 g . It is evident that the experimental data at the top of the columns appear to be approaching the predicted curve in the appropriate time sequence. At the bottom, the solid content appears to be too great. This arises, not because of a failure in the theory, but because of the failure of the assumption that particle sorting does not occur. The red mud has a small amount of sand-sized material present despite initial thickening by cyclone. This sand tends to accumulate at the bottom of the equilibrating column of colloid and hence reduces the water content there.

Sieve analysis confirms that sorting does occur. For convenience a 0.003-mm sieve was used. This separates the international fine- and coarse-sand fractions, but leaves the silt. For duplicate samples centrifuged for 4 hr, 15% (on a dry mass basis) of this material was found in the bottom section (0 to 0.25 mm), about 1% in the 0.25 to 0.75 mm section, and a negligible amount thereafter. It is interesting that the sand had a density of $2.5 \times 10^3\text{ kg/m}^3$ and hence was significantly less dense than the average for the mud, $3.2 \times 10^3\text{ kg/m}^3$.

A further series of experiments was therefore performed. In this series the coarser material was removed by centrifuging for 1 hr and discarding the material in the lowest $5 \times 10^{-3}\text{ m}$ section. The remaining solid was redispersed in the supernatant liquid and the sedimentation or filtration experiment performed as above for 4 hr. The results are shown in Fig. 7(b). The experimental profiles are consistent with prediction, bearing in mind that the columns are probably still equilibrating.

Figure 8 shows the corresponding data for the self-weight filtration. It will be noted that the predicted "equilibrium" profiles are drier throughout than the corresponding profiles shown in Fig. 7. The experimental data are consistent with this prediction. These data, however, require a little more explanation than those for Fig. 7. During the early stages of self-weight filtration, liquid separation from the slurry in this material occurs not only at the bottom of the column, but also at the top. This phenomenon has been described in a semiquantitative way by Smiles (14). It implies that until the free water is removed from above the settling sample, the water potential at the top will be zero and the water content correspondingly great. When this water is removed, however, the surface rapidly experiences values of Ψ appropriate to the filtration situation. This phenomenon is observed in the experimental data in Fig. 8(a) where the 30-min profile has free water standing above it and a wet surface while the 4-hr profile has

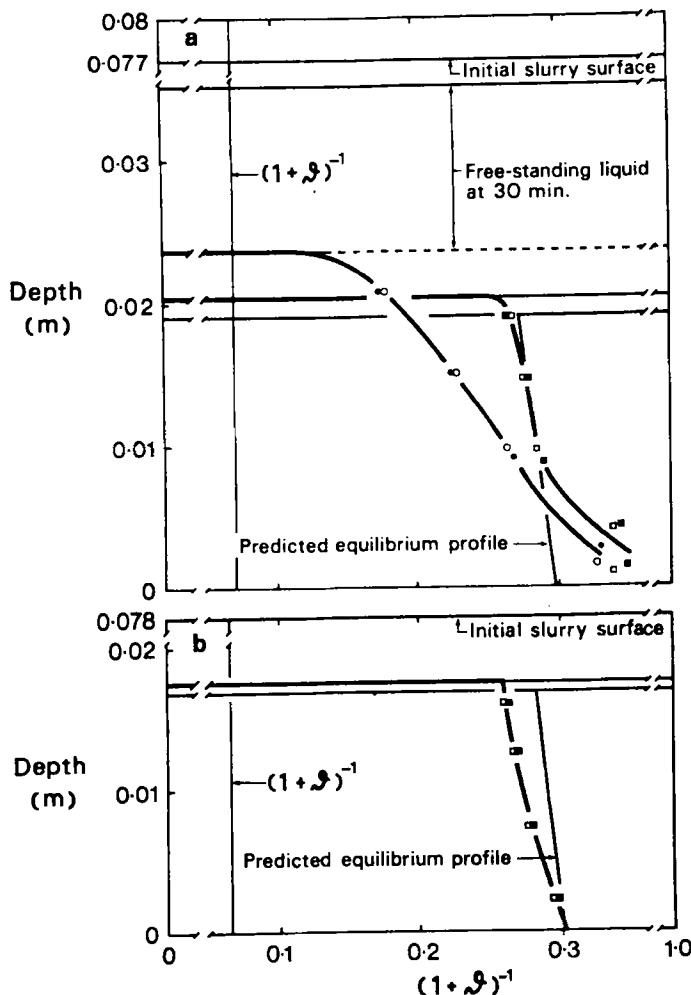


FIG. 8. Profiles corresponding to Fig. 7, but with liquid escape permitted through the base of column.

drained. The anomalously low water contents at the base of these profiles (Fig. 8a) are accompanied by an increase in sand similar to that observed in sedimentation. The data of Fig. 8(b) (corresponding to Fig. 7b data) agree within experimental error with prediction. Finally, it should be noted that some cracking occurred in the 4-hr profile. The theory presented here strictly applies only to two-phase situations, but the limited cracking observed should only marginally affect the predicted liquid/solid distribution.

APPLICATION TO OTHER MATERIALS

As we noted in the theoretical section, this approach to the prediction of equilibrium profiles depends on there being an experimentally determinable $\Psi(\vartheta)$ relation for a slurry. All porous materials over some ϑ in the range $0 \leq \vartheta \leq \vartheta_{\max}$ will reveal such a relation, and in this range ϑ profiles will be predictable, provided that the material has an effectively restricted particle size range.

Not all materials, however, will have a $\Psi(\vartheta)$ of the form shown in Fig. 2. For example, the moisture characteristic of a phosphate slime produced during the extraction of rock phosphate and supplied by Broken Hill South Ltd., an Australian mining company, appears to be describable in terms of the equation

$$\vartheta = \alpha(-\Psi/100)^\beta \quad (16)$$

in which $\alpha = 1.373$ and $\beta = -0.189$.

The use of this equation together with Eqs. (10) and (13) shows that, in general, phosphate slime behaves similarly to red mud so far as the effects of ϑ_n , T_n , and Z are concerned.

The form of Eq. (16) is interesting. If $\beta = -1$, it has the form of the equation for colloid osmotic pressure which Philip (15, 16) contends is appropriate for sufficiently dilute colloidal suspensions. In this case there is never a clear interface between the liquid and the sedimenting solid, no matter how dilute the initial slurry. Equations (15) and (16) with $\beta \neq -1$ both imply a clearly defined surface to the sediment even though ϑ there approaches infinity. The equilibrium distributions of solid in these cases are independent of ϑ_n and depend only on M .

Finally, it should be noted that while Eqs. (15) and (16) are convenient for use in the analyses presented here, it is by no means clear (cf. Ref. 3) that all materials will have $\Psi(\vartheta)$ of a form describable in terms of simple functions. For such materials, numerical integration will be necessary.

Again, the known forms of $\Psi(\vartheta)$ are consistent in general with the results obtained using Eq. (15).

CONCLUSION

The experiments described here are in some respects a compromise since we seek to test a theory with some particular assumptions and at the same time describe the properties of a significant industrial effluent. The effluent as it was received fails to satisfy the assumption that the particle size and density be sufficiently restricted that sorting does not occur. The profiles of water and solid content observed are, however, consistent with the theory if the settling of some coarse material is accepted, and if it is assumed that this coarse material does not materially affect the $\Psi(\vartheta)$ relations of the essentially colloidal system. If coarse material is removed, the agreement is excellent. It is noted, however, that equilibrium profiles do not provide a good test of the theory. This must await solutions of the nonlinear Fokker-Planck equation describing flow of the liquid in a Lagrangian coordinate system.

The theory does, however, permit prediction of the relative efficacy of some strategies that might be adopted for using gravity to dewater some slurries.

It is evident that best recovery of liquid will be obtained when the free water surface with which the slurry equilibrates is maintained as low as possible. It is also shown that for slurries of the same water content, increasing the initial depth, and hence the total solid content, will increase the ultimate liquid recovery per unit volume of slurry (or solid). These results are general for all materials satisfying the assumptions of the theory and having a determinable $\Psi(\vartheta)$. Of course, the most satisfactory ultimate recovery does not indicate the most desirable strategy. However, this can be determined in terms of rates of liquid recovery and the evolution of the ϑ profiles, given by solutions to the flow equation. Some appropriate solutions will be published shortly, but it is worth noting that the early stages of filtration may be predicted using T_n , ϑ_n , and the data of Fig. 2, using an approach of Smiles (17).

Finally, we note that the use of a centrifuge implies that the theory carries over to this form of particle/liquid separation, with the restriction that the flow equation (6) has not yet been extended to two or three dimensions. The variation of g with z complicates the calculation of the equilibrium profile which must be calculated in z space rather than m , but no conceptual difficulties are involved.

SYMBOLS

ϑ	volumetric liquid content per unit volume of solid (m^3/m^3)
Ψ	liquid potential (m liquid)
P_1	manometric pressure (m liquid)
P	total pressure (m liquid)
T	upper surface of system (m)
γ	wet specific gravity of slurry
V	volume flux of liquid relative to solid (m^3/m^2 sec)
K	hydraulic conductivity of material (m/sec)
Φ	total potential of liquid (m liquid)
Z	height datum (m) set for convenience at surface of equilibrium free water
m	material (Lagrangian) coordinate (m)
t	time (sec)
D_m	diffusivity in Lagrangian coordinates (m^2/sec)
ρ_c	solid specific gravity
K_m	hydraulic conductivity in Lagrangian coordinates (m/sec)
M	length (fixed) of system in Lagrangian coordinates (m)
α, β	constant coefficients

REFERENCES

1. G. J. Kynch, *Trans. Faraday Soc.*, **48**, 166 (1952).
2. E. B. Fitch, *Trans. AIME*, **223**, 129 (1962).
3. C. C. Dell and W. T. H. Kelleghan, *Powder Technol.*, **7**, 189 (1973).
4. G. K. Batchelor, *Ann. Rev. Fluid Mech.*, **6**, 227 (1974).
5. K. Terzaghi, *Theoretical Soil Mechanics*, Wiley, New York, 1943.
6. I. K. Lee and I. B. Donald, in *Soil Mechanics Selected Topics* (I. K. Lee, ed.), Butterworths, Sydney, 1968, pp. 58-81.
7. J. R. Philip, *Aust. J. Soil Res.*, **7**, 99 (1969).
8. J. R. Philip, *Water Resour. Res.*, **6**, 1248 (1970).
9. D. E. Smiles and A. G. Harvey, *Soil Sci.*, **116**, 391 (1974).
10. A. McNabb, *Q. Appl. Math.*, **17**, 337 (1960).
11. P. A. C. Raats and A. Klute, *Soil Sci. Soc. Am., Proc.*, **32**, 161 (1968).
12. D. E. Smiles and M. J. Rosenthal, *Aust. J. Soil Res.*, **6**, 237 (1968).
13. E. J. Buckingham, *U. S. Dep. Agric., Bull.*, **38** (1907).
14. D. E. Smiles, *Separ. Sci.*, **10**, 767 (1975).
15. J. R. Philip, *J. Chem. Phys.*, **52**, 1387 (1970).
16. J. R. Philip, *Soil Sci.*, **109**, 294 (1970).
17. D. E. Smiles, *Ibid.*, **117**, 288 (1974).

Received by editor April 12, 1975